

Preliminary calibration results of the HY-2B altimeter's SSH at China's Wanshan calibration site

Chuntao Chen^{1*}, Jianhua Zhu², Chaofei Ma³, Mingsen Lin³, Longhao Yan², Xiaoqi Huang², Wanlin Zhai², Bo Mu³, Yongjun Jia³

¹ School of Ocean, Yantai University, Yantai 264005, China

² National Ocean Technology Center, Ministry of Natural Resources, Tianjin 300112, China

³ National Satellite Ocean Application Service, Ministry of Natural Resources, Beijing 100081, China

Received 20 August 2020; accepted 25 December 2020

© Chinese Society for Oceanography and Springer-Verlag GmbH Germany, part of Springer Nature 2021

Abstract

Satellite altimeter needs to be calibrated to evaluate the accuracy of sea surface height data. The dedicated altimeter calibration field needs to establish a special calibration strategy and needs to evaluate its calibration ability. This paper describes absolute calibration of HY-2B altimeter SSH using the GPS calibration method at the newly Wanshan calibration site, located in the Wanshan Islands, China. There are two HY-2B altimeter passes across the Wanshan calibration site. Pass No. 362 is descending and the ground track passes the east of Dan'gan Island. Pass No. 375 is ascending and crosses the Zhiwan Island. The GPS data processing strategy of Wanshan calibration site was established and the accuracy of GPS calibration method of Wanshan calibration site was evaluated. Meanwhile, the processing strategies of the HY-2B altimeter for the Wanshan calibration site were established, and a dedicated geoid model data were used to benefit the calibration accuracy. The time-averaged HY-2B altimeter bias was approximately 2.12 cm with a standard deviation of 2.08 cm. The performance of the HY-2B correction microwave radiometer was also evaluated in terms of the wet troposphere path delay and showed a mean difference -0.2 cm with a 1.4 cm standard deviation with respect to the *in situ* GPS radiosonde.

Key words: calibration, HY-2B, altimeter, Wanshan calibration site, GPS buoy

Citation: Chen Chuntao, Zhu Jianhua, Ma Chaofei, Lin Mingsen, Yan Longhao, Huang Xiaoqi, Zhai Wanlin, Mu Bo, Jia Yongjun. 2021. Preliminary calibration results of the HY-2B altimeter's SSH at China's Wanshan calibration site. *Acta Oceanologica Sinica*, 40(5): 129–140, doi: 10.1007/s13131-021-1745-y

1 Introduction

The HY-2B satellite was launched on October 25, 2018 from Taiyuan, China as a follow-on to the HY-2A satellite. It is the first operational ocean dynamic satellite to form a satellite constellation with the subsequent satellite HY-2C (scheduled to be launched between the end of 2020 and the beginning of 2021) and HY-2D (after 2022) for maritime dynamic environmental monitoring. Similar to the HY-2A, four microwave instruments were carried into space by the HY-2B satellite, including a Ku and C band altimeter, a Ku-band scatterometer, a scanning microwave radiometer, and a three-frequency correction microwave radiometer. Unlike HY-2A, HY-2B is also equipped with an automatic identification system (AIS), which can detect, demodulate and forward AIS messages and a data collection system (DCS), which can receive buoy measurement data from China's offshore and other sea areas, and transmit the data after storing through the satellite digital transmission channel (Lin et al., 2019). As an ocean dynamic satellite, HY-2B altimeter can cover 90% of the world's oceans and provide all-weather and all-time observations with a design life of 5 years, and will provide directly significant wave height (SWH), sea surface height (SSH), sea surface wind (SSW) data on a global scale (Lin et al., 2019). The SSH data, one of the most important parameters obtained by the HY-2B altimeter, can be extensively utilized in oceanography,

geophysics and geodesy (Chen, 2010; Fu and Cazenave, 2001; Ma et al., 2020). The most important application of altimeters is to monitor global sea level rise, which requires a high-precision SSH measurement data of the altimeter (Frappart et al., 2015).

Calibration of the altimeter missions plays a key role in terms of accuracy of the raw satellite measurements, and extends the applications of altimetry data. The biases, errors and drifts of an altimetry system's performances must be continuously monitored and corrected by the absolute calibration. Absolute calibration of altimeters is achieved by dedicated facilities, which are independent of satellite altimeter system (Mertikas et al., 2018). These dedicated calibration sites on ground can monitor the altimetry measurements continuously, and ensure the succession from one altimeter mission to the follow-up mission in a same calibration method and benchmark (Mertikas et al., 2018).

Up to now, there have been four absolute, permanent and historic calibration sites all over the world. Corsica, which was established in 1998, is running by the French space agency CNES in Corsica, France (Bonnetfond et al., 2003a, b, 2010, 2015, 2018; Cancet et al., 2013). It supports continuous monitoring of Jason-2 and Jason-3 (formerly T/P and Jason-1), and Sentinel-3A and SARAL/ALtiKa (formerly ERS and Envisat). It is equipped with four pressure tide gauges leveled to a permanent GPS receiver. Harvest oil platform calibration site is operated by the Jet Propul-

Foundation item: The National Key R&D Program of China under contract Nos 2018YFB0504900 and 2018YFB0504904; the National Natural Science Foundation of China under contract Nos 41406204 and 41501417; the Operational Support Service System for Natural Resources Satellite Remote Sensing under contract No. 180019.

*Corresponding author, E-mail: chenchuntao@ytu.edu.cn

sion Lab (JPL)/National Aeronautics and Space Administration (NASA) in California, USA in 1992 (Haines et al., 2010, 2016). It is mainly equipped with a GPS station, an up-looking water vapor radiometer, and three tide gauge systems. Bass Strait is run by the University of Tasmania in Bass Strait, Tasmania, Australia in 1992. It is mainly equipped with two GPS buoy, two GPS stations, and two tide gauge systems (Watson et al., 2003, 2011, 2016). The Gavdos calibration site is managed by the Technical University of Crete in Greece in 2004. It is mainly equipped with 17 permanent Global Navigation Satellite System (GNSS) stations, eight tide gauges, six meteorological systems, several communication links, and one microwave transponder (Mertikas et al., 2010, 2016, 2018). These calibration facilities are all for Jason-1, Jason-2, Jason-3 and Sentinel-3A in the oceans.

China has launched two marine dynamic environmental satellites that embark altimeters, and will launch at least two other altimeter satellites in the coming 5 years, forming a constellation with the HY-2B for maritime environmental monitoring. For this reason, a dedicated calibration site is imperative and important. A vessel survey campaign was implemented during March 2018 and acquired the geoid slope and water depth in the sea area at the Wanshan calibration site. Based on the survey campaign, a nested Wanshan calibration tide model was established, and its accuracy has been assessed through a tide gauge and GPS buoy. In 2019, tide gauges, four GPS Reference Stations (GPSRS) and a weather station were built.

The accuracy of HY-2B SSH is the focus of remote sensing application experts and international peers. The absolute calibration of HY-2B is the precondition for the joint use of HY-2B data with other altimeters. The calibration capability of China's dedicated altimeter calibration field, which was basically completed in 2019, is also the main issue of international altimeter calibration team. This paper introduces the composition of the Wanshan altimeter calibration site in China, the HY-2B in-orbit calibration campaign carried out at the Wanshan calibration site, and two later HY-2B altimeter calibration experiments. The GPS absolute

calibration method of Wanshan calibration site was described, which included the calibration accuracy of GPS buoy system in Wanshan calibration field, and the altimeter data processing strategy specially designed for Wanshan calibration field. Section 2 presents the Wanshan calibration site, HY-2B altimeter data, the error budget for GPS buoy measuring system, the GPSRS and the calibration methodology, followed by a description of the GPS SSH and altimeter SSH calculation formulas. Section 3 discusses the calibration results, including the accuracy of wet troposphere path delay correction (WTPD) for the HY-2B correction microwave radiometer (CMR) and absolute biases in the HY-2B altimeter SSH. Section 4 presents a discussion and Section 5 is conclusions.

2 Materials and methods

This paper used the shipboard GPS buoy at the Wanshan calibration site to calculate the absolute bias in the HY-2B altimeter SSH. The Pass No. 362 is descending and the ground track passes the east of Dan'gan Island. Pass No. 375 is ascending and crosses the Zhiwan Island. So two GPSRSs, one was setup in the Dan'gan Island and another was in the Zhiwan Island, were used for the GPS buoy solution. Before the calibration experiments, the accuracy of GPS buoy to measure SSH was evaluated using the tide gauge data of the Zhiwan Island.

This research can also be regarded as a feasibility and accuracy evaluation of the GPS buoy calibration method for the Wanshan calibration site. In 2018 and 2019, two campaigns to estimate the absolute bias of the HY-2B altimeter were organized over this calibration site, and a total of eight *in situ* measurements were collected and processed.

2.1 Description of the Wanshan calibration site

The Wanshan calibration site is located in the north of the South China Sea (SCS) near Hong Kong (Fig. 1). Currently owned and operated by the National Satellite Ocean Application Service,

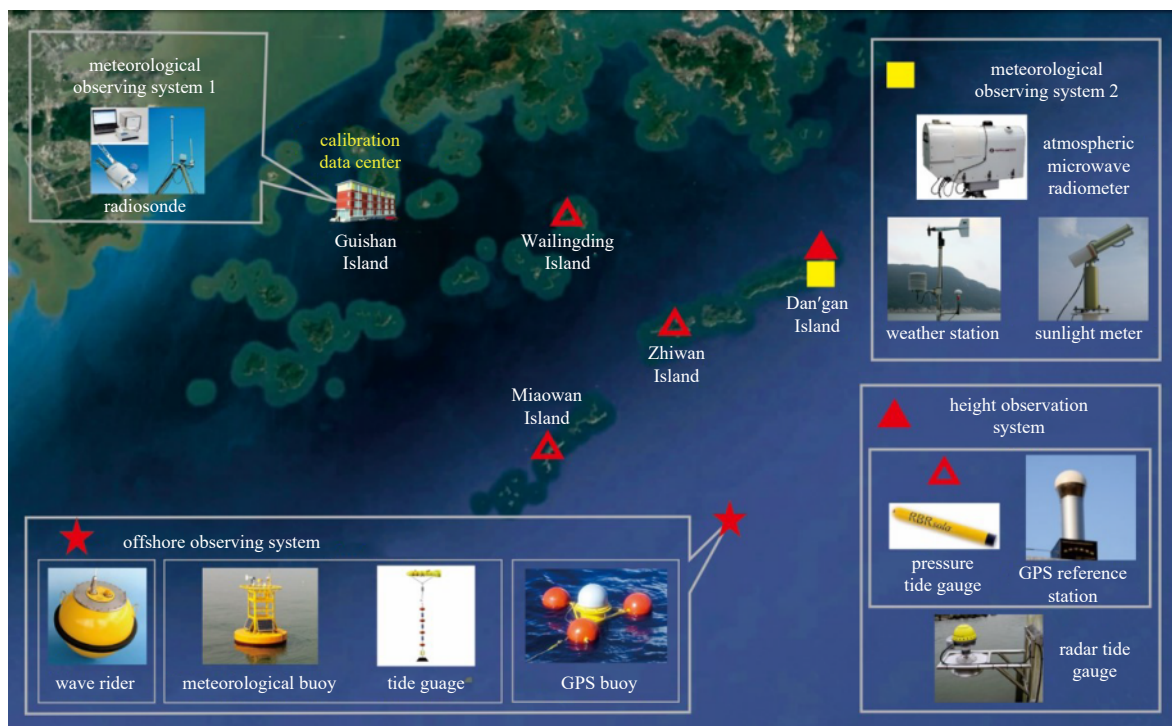


Fig. 1. Functional components of the Wanshan calibration site.

Ministry of Natural Resources of the People's Republic of China, the site is composed of the Dan'gan Island (DG), Zhiwan Island (ZW), Miaowan Island (MW) and Wailingding Island (WLD). There will be three distinct methods at the Wanshan calibration site for measurement of the *in situ* SSH at the comparison point: the tide gauge method, GPS buoy method and mooring tide gauge method. The primary water-level sensors are tide gauges located at DG, ZW and WLD, each of which is equipped with a GPS station to monitor the vertical movement and provide the accurate reference height of the tide gauges. The fourth tide gauge will be installed at the MW site as designed. GPS data are also used for computing and correcting the wet troposphere path delay measurements of altimeter (red triangle in Fig. 1).

The GPS buoy and mooring tide gauge will be deployed in the sea approximately 20 km off the coast of ZW (yellow square in Fig. 1). A weather station was installed at DG in 2019, near the GPSRS. The main purpose of this weather station is to measure atmospheric pressure, which can be used to correct the pressurized tide gauge and the altimeter dry tropospheric path delay.

The principle of the tide gauge calibration methodology shown in Eq. (1) is to calculate the difference between altimeter SSH and tide gauge SSH recorded near the coastal. These two SSHs are located in two places with a certain distance. The link between the two SSHs is mostly the geoid slope and partly the differential tides from the altimetry nadir point to the coastal tide gauge locations.

$$\text{Bias} = \text{SSH}_{\text{alt}} - \text{SSH}_{\text{tide gauge}} - \text{Geoid_Difference} - \text{Tidal_Difference}. \quad (1)$$

A dedicated GPS towing-body campaign was launched in 2018 to determine a geoid slope approximately 28 km long and 8 km wide centered on the HY-2B altimeter ground track. The geoid slope between the ZW site and surrounding the offshore altimeter comparison point was computed in 2018 (Fig. 2) using a GPS towing body, which was used to calculate the bias in Eq. (1) (Zhai et al., 2020). The geoid slope of the Wanshan calibration site is abbreviated here to WGeo.

To guarantee the WGeo accuracy, check lines more than 50 km long were designed. Approximately 5 d of vessel towing measurements allowed us to cover an ocean area surface of more than 200 km². The results showed that the precision of WGeo was at the level of 2 cm. More details are presented in Zhai et al. (2020).

A precise tide model was also needed to measure the difference caused by tides, as can be seen from Eq. (1). The four dedicated operational calibration sites do not need a tide model, partly because there is little variation in the tides at Gavdos and Corsica (Mertikas et al., 2018; Bonnefond et al., 2003a, b), and partly because the *in situ* instruments are exactly at the comparison point, as for example, at the Harvest and Bass Strait sites. However, at the Wanshan calibration site, the tidal difference between the comparison point and the coastal tide gauge is not negligible (approximately 4–5 cm standard deviation (STD) in the daytime) and so a precise and stable tide gauge is necessary.

A numerical model was established for the two layers nested in the Zhujiang River Estuary and the surrounding sea area. The Zhujiang River Estuary and the northern shelf area of the SCS cover large areas (Fig. 3a), and the vertical boundary of the grid extends approximately 200 km outward with a horizontal resolution of 1 km. The grid for small areas (Fig. 3b) was nested with a 1:5 encryption coefficient and a horizontal resolution of 0.2 km.

The accuracy of the tide model was accessed using a GPS

buoy and tide gauge measurements. The specific method is described here. First, a tide gauge was used to measure the sea level change over a period of time. Next, a GPS buoy was deployed to measure the sea level change at the altimeter comparison point on the sea during the same time period as the tide gauge. Then the tide model established was used to perform a tidal simulation of the Wanshan calibration site during the test to obtain the tidal difference between the coastal tide gauge and the offshore altimeter comparison point. Finally, the tidal difference measured by the tide gauge and the GPS buoy was used to evaluate the accuracy of the tidal difference at the two points from the tide model simulation. The final results showed that the accuracy of the tidal difference simulated by the tide model was better than 1.5 cm.

In this paper, the GPS buoy calibration method is used and the tidal difference between the GPS buoy position and altimeter point is negligible. Specific calculation methods and results will be described in detail in a later article.

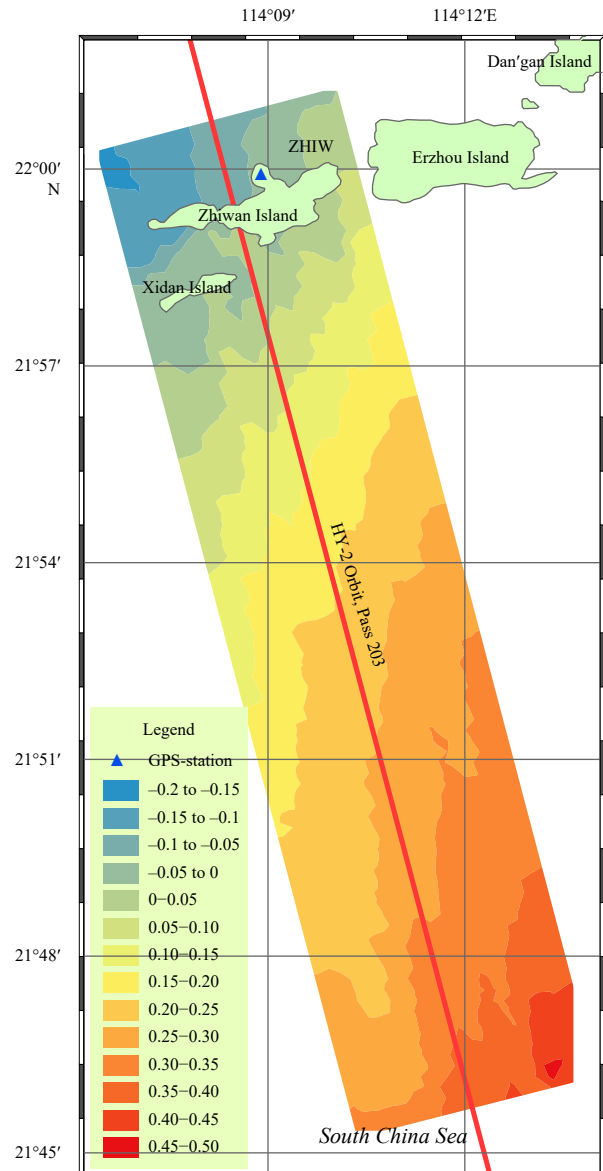


Fig. 2. Wanshan geoid slope acquired from the 2018 vessel survey campaign (Zhai et al., 2020).

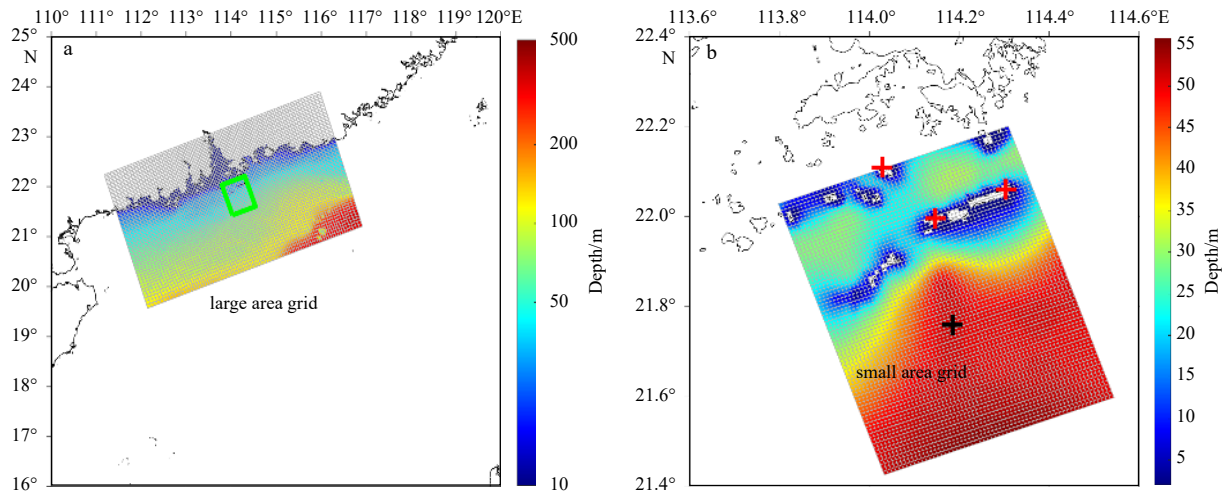


Fig. 3. Nested Wanshan calibration tide model. a. A large tide model was established to provide tide data as boundary conditions for the small area tide model. b. Small area grid was used in the Wanshan precise tide model.

2.2 Calibration data

The equipment used to collect the data set for HY-2B calibration included the HY-2B altimeter, GPS buoy, GPSRS and GPS radiosonde. The dedicated GPS buoy (shown in Fig. 2 in Chen et al. (2019)) was designed for altimeter SSH calibration and the GPSRS in this paper are briefly presented.

2.2.1 HY-2B altimeter

On October 25, 2018, the HY-2B mission was successfully launched as a continuation of the HY-2A mission. The HY-2B altimeter data used in this study were level 2 interim geophysical data records (IGDR) distributed by the National Satellite Ocean Application Service, Ministry of Natural Resources of the People's Republic of China. The HY-2B altimeter is a nadir-looking pulse-limited altimeter operating on two frequency bands, the Ku band (13.58 GHz) and the C band (5.25 GHz), with a limited pulse footprint of 2 km. A CMR is also included in the HY-2B payload, with the major objective of providing atmosphere WTPD corrections for the accompanying altimeter. It operates on three frequencies: 18.7 GHz, 23.8 GHz and 37.0 GHz. The nominal satellite altitude of approximately 971 km with an inclination of 99.340 15 and an orbit repeat time of 14 d provides observations of the earth's surface (ocean and land) from 80.70°N to 80.70°S, formerly covered by the HY-2A altimeter, with an equatorial ground-track spacing of approximately 207.64 km. The target SSH accuracy over the oceans is approximately 5 cm.

For the HY-2B altimeter, the IGDR data were 1-Hz data and adopted, as shown in Table 1, Row 2.

2.2.2 GPS buoy

The GPS buoy can be used directionally to measure sea level in the same reference frame as the altimeter measurement. The GPS buoy calibration method that was used in this study is a purely geometric relationship between altimeter SSH and deployed GPS buoy. The GPS buoy is mainly composed of a floating platform equipped with three float balls, a choke ring antenna with a dome and a GPS receiver. The GPS buoy that was used for HY-2B calibration in this work was designed in 2013. In the buoy design stage, the GPS buoy's wave-following performance, the influence of the antenna height on the height measurement, and the stability of the buoy body (roll angle and heave rate with the ocean wave) were analyzed through a hydrodynam-

Table 1. Sources of the main parameters for HY-2B altimetry measurement

Parameter	HY-2B
Institution	NSOAS, MNR
Vision	HY-2B IGDR
Dry troposphere correction	National Centers for Environmental Prediction
Wet troposphere correction	HY-2B CMR
Ionosphere correction	HY-2B Altimeter
Pole tide	Wahr 1985 model
Solid earth tide	Cartwright and Tayler model
Ocean load tide	GOT4.10c
Geoid	EGM2008/WGeo

ics numerical simulation. After the successful manufacture, through the laboratory water tightness test, the field antenna height measuring, the hydrostatic height measurement test and the GPS reference station distance influence experiment, the accuracy of the GPS buoy measurement system to measure the water level height was finally obtained and more details were given in Chen et al. (2014, 2019). In this paper, only the accuracy of GPS buoy measurement is summarized. GPS processing for the altimeter calibration included two main steps. Firstly, the positions of the GPS reference stations were resolved in a global terrestrial reference frame (ITRF 2008) and then transferred to the HY-2A and Jason-2 reference frame. This first step ensured that the SSH data measured by the GPS buoy had the same reference frame as the SSH from the altimeters. The second step used the real-time kinematic (RTK) technique to acquire the sea level of the GPS buoys on a continuous basis during GPS buoy deployment at the altimeter nadir point.

The SSH measurement error budget for the GPS buoy is shown in Table 2. The GPSRS is about 25 km distance from the deployed GPS buoy at the Wanshan calibration site, the total error is better than 3.0 cm RMS for the SSH measured by GPS buoy.

In the calibration campaign in November 2018, a tide gauge was used to perform a comparison experiment on the GPS buoy. A Lowess filter was used (300 points sliding and smoothing in 5 min) in the tide gauge data processing, and the reference ellipsoid height of the tide gauge was obtained from the ZW GPSRS. The SSH at the GPS buoy was calculated using the method given in Chen et al. (2014, 2019). Finally, the SSH at the tide gauge in

Table 2. Error budget for GPS buoy SSH measurement

	Error source	Accuracy/cm
GPSRS	static solutions	<1.0
	antenna height and PCV	0.2
GPS buoy SSH	antenna PCV	0.2
	antenna height to water level	<0.1
	kinematic solution	<2.5
GPS totals:		<2.7

Note: PCV represents phase center variation.

the same coordinate frame as the GPS buoy was used to evaluate the accuracy of the SSH at the GPS buoy (Fig. 4)

The difference of the GPS buoy sea level and tide gauge sea level was approximately 0.66 cm STD in the experiment, which involved approximately 4 h of comparison. The distance between the GPSRS and the GPS buoy was approximately 500 m; the dis-

tance in altimeter SSH calibration experiments is usually 25 km, so the effect of this distance on the solution for the SSH at the GPS buoy should be accounted for. Using kinematic processing techniques, a 10 km increase in distance gives a 1 cm increase in the error, so the accuracy of the SSH at the GPS buoy was approximately 2.59 cm. The accuracy of the SSH at the GPS buoy accessed by the comparison experiment is consistent with the accuracy of the GPS buoy measurement of < 2.7 cm given in Table 2.

2.2.3 GPSRS

Two GPSRSs were deployed at the Wanshan calibration site: one at the ZW station and another at the DG station (Fig. 1 and Table 3). For the ZW and DG stations, the raw data set covered 40 d (November 3 to December 12, 2018) during the first campaign and 6 d (September 27 to October 2, 2019) during the second campaign. The sample rate was set to 1 s during both campaigns.

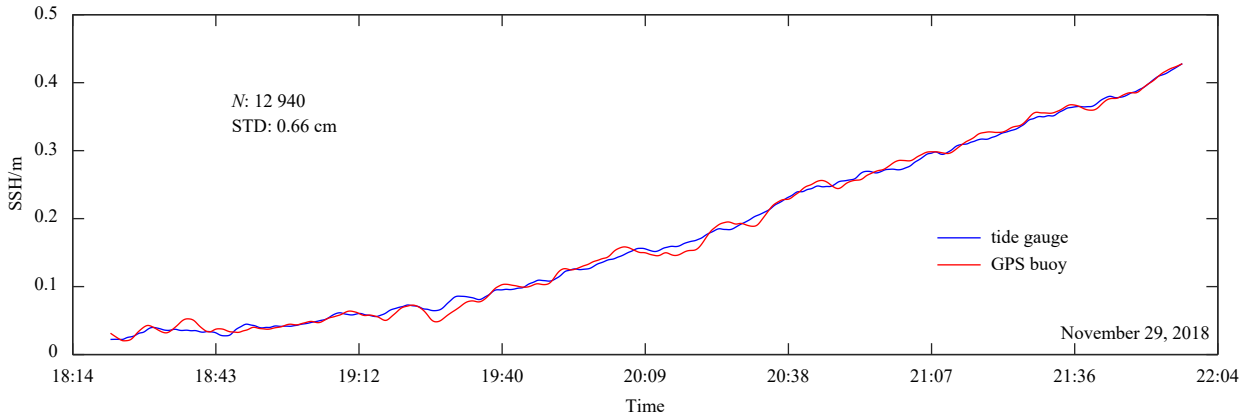


Fig. 4. Accuracy of the SSH at the GPS buoy assessed by the tide gauge. STD is standard deviation and *N* is the number of samples.

The GPS station consisted of a GPS receiver (Trimble Net R9), a choke ring antenna (Trimble 59 800) and an antenna dome. The receive frequency of GPSRS is 1-s intervals during the campaign (Table 3) to support kinematic GPS processing.

To calculate the SSH at the GPS Buoy, the absolute positions of the GPSRSs need to be calculated first, which are then transferred to the HY-2B altimeter reference frame ($\Delta H_{ref \text{ buoy alt}}$ in Eq. (10)). The HY-2B altimeter data are provided on an ellipsoid with an inverse flattening of 298.257 and a semi-major axis of 6 378 136.3 m, while the GPS output is on a difference ellipsoid with an inverse flattening of 298.257 and a semi-major axis of 6 378 137.0 m.

The GPSRSs were solved using GAMIT/GLOBK software (King and Bock, 2005), which was developed by the Massachusetts Institute of Technology, to get the absolute positions. The TEQC software (Estey and Wier, 2013) was used to make quality control for the GPSRS data. The GPSRS data were processed in combination with the nearby International GNSS Service (IGS) stations. The IGS includes over 400 GNSS stations distributed around the world, and provides GNSS orbits, tracking data, and other high-quality GNSS data, products and services online in

near real time. A total of 27 IGS stations (Fig. 5) were processed together with the GPSRSs, which were installed at Wanshan calibration site using the GAMIT/GLOBK software (version 10.60) in this research (Herring, 2002; Herring et al., 2018a, b).

The following simple formula illustrates the principle used to resolve the GPSRS position.

$$\begin{bmatrix} X \\ Y \\ Z \end{bmatrix}_{\text{GPS reference station}} = \begin{bmatrix} X_0 \\ Y_0 \\ Z_0 \end{bmatrix}_{\text{IGS}} + \begin{bmatrix} \Delta X \\ \Delta Y \\ \Delta Z \end{bmatrix}, \quad (2)$$

where $\begin{bmatrix} X \\ Y \\ Z \end{bmatrix}$ is the GPSRS position which needs to be acquired and $\begin{bmatrix} X_0 \\ Y_0 \\ Z_0 \end{bmatrix}$ is the 27 IGS positions, which are known accurately.

With the precise positions of the GPSRSs resolving, the TRACK was used to calculate the SSH of the GPS buoy through the real-time kinematic (RTK) processing techniques during the GPS buoy deployment at the point of HY-2B altimeter ground track (Herring, 2002). The TRACK is a kinematic GPS positioning software, which now is used for GPS resolution and firstly used for airborne laser altimetry applications.

2.2.4 GPS radiosonde

The WTPD correction plays an important role in the preci-

Table 3. Location and time of observation for each GPSRS

Station name	Location	Start time	End time
ZW	Zhiwan Island	03/11/2018	12/12/2018
DG	Dan’gan Island	03/11/2018	12/12/2018
ZW	Zhiwan Island	27/09/2019	02/10/2019
DG	Dan’gan Island	27/09/2019	02/10/2019

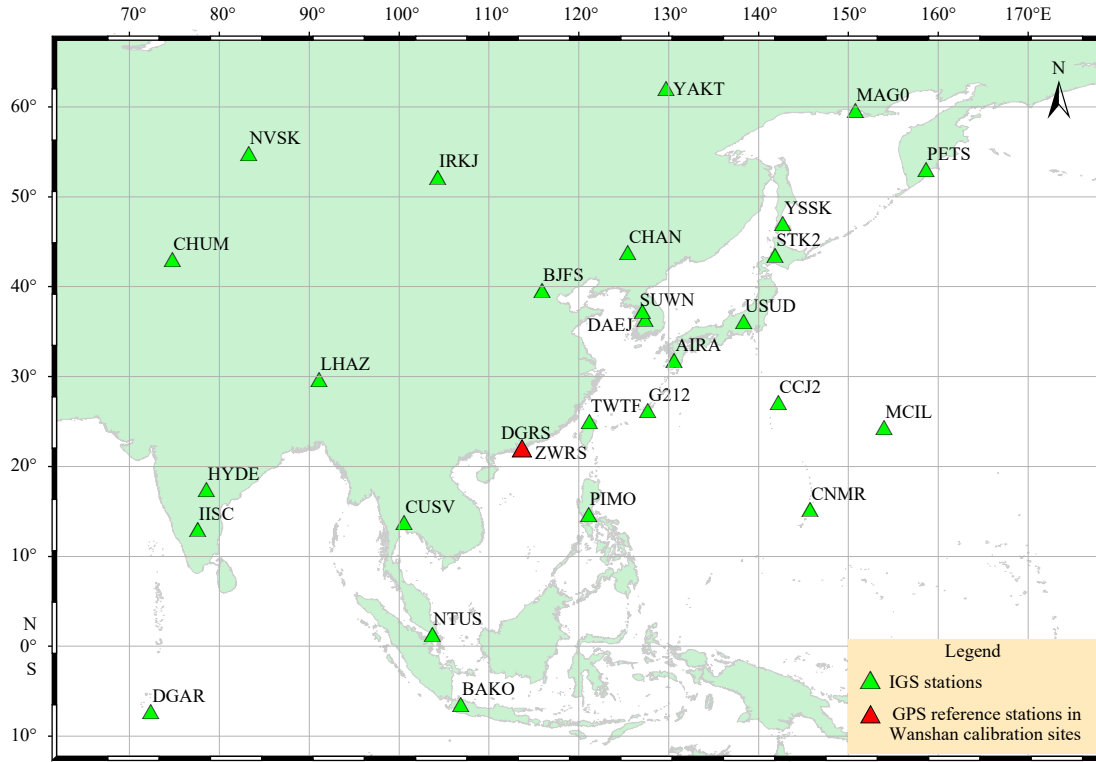


Fig. 5. International GNSS Service (IGS) stations were selected to solve the GPS reference stations (GPSRSs) for the statistical data solution. The red triangle represents the Wanshan GPSRSs (DG reference station and ZW reference station). The green triangles represent the IGS stations.

sion SSH measurements provided by a satellite altimeter, so an onboard microwave radiometer is installed on the satellite to derive the WTPD for ocean altimetry, such as TMR (Topex/Poseidon microwave radiometer), JMR (Jason microwave radiometer), AMR (Jason-2/3 advanced microwave radiometer), CMR (HY-2A calibration microwave radiometer) and MWR (Envisat microwave radiometer) (Keihm et al., 1995; Brown et al., 2004; Brown, 2010; CLS, 2013; Zheng et al., 2014). However, in the nearshore zone, the microwave radiometer is affected by the footprint of the land, producing a problem with missing or inaccurate data, and for this reason, calibration of the altimeter is always done at an ocean calibration site that is built near the coast and supported by land-based laboratories. To conduct accurate altimeter calibration and successfully calibrate the WTPD of the altimeter, a GPS radiosonde was used to evaluate the WTPD of the HY-2B altimeter in this research.

The WTPD includes contributions from both the liquid water content of the clouds and water vapor. However, the value of the path delay caused by the liquid water content is less than 1 mm, which is 1–2 orders of magnitude smaller than the effect of water vapor under no-rain conditions, and thus the WTPD can be written as:

$$\Delta R_{\text{wet}} = 10^{-6} \int_0^h N_{\text{vap}}(z) dz = 1.763 \times 10^{-3} \int_0^h \frac{\rho_{\text{vap}}(z)}{T(z)} dz, \quad (3)$$

where R_{wet} is path delay of vapor, N is the refractivity, defined to be the difference between the index of refraction on the atmosphere and in the water vapor, z is in m. T is the air temperature (K), ρ_{vap} is the water vapor density (g/cm^3), and h is the maximum height of observation.

The water vapor density cannot be acquired directly from the GPS radiosonde, so the general gas equation was used to calculate it.

$$\rho_{\text{vap}} = \frac{P_v M}{RT}, \quad (4)$$

where P_v is the vapor pressure (Pa), R is the ideal gas constant ($\text{J}/(\text{K}\cdot\text{mol})$) and M is the molar mass of water (g/mol).

Then, the WTPD can be calculated as:

$$\Delta R_{\text{wet}} = 1.763 \times 10^{-3} \int_0^h \frac{P_v(z) M}{RT(z)^2} dz. \quad (5)$$

2.3 Calibration methodology

The absolute calibration of satellite altimeters has been mainly provided by GPS buoy methodology and tide gauge methodology (Mertikas et al., 2018; Frappart et al., 2015; Bonnefond et al., 2017; Haines et al., 2016; Watson et al., 2016; Chen et al., 2019). The Wanshan calibration site was designed to use both methodologies, but because the site is now in the test phase, only the GPS buoy methodology is presented in this article. Pass No. 362 is descending and the ground track passes the east of Dangan Island. Pass No. 375 is ascending and crosses the Zhiwan Island (Fig. 6).

The calibration methodology was the same as used at the Qinglan Port (Chen et al., 2019), which was the site used to estimate the accuracy of the Jason-2's SSH and HY-2A altimeter's SSH with the same GPS buoy. Using the same GPS buoy, the altimeter bias estimate was about -2.3 cm for the Jason-2 Geophysical

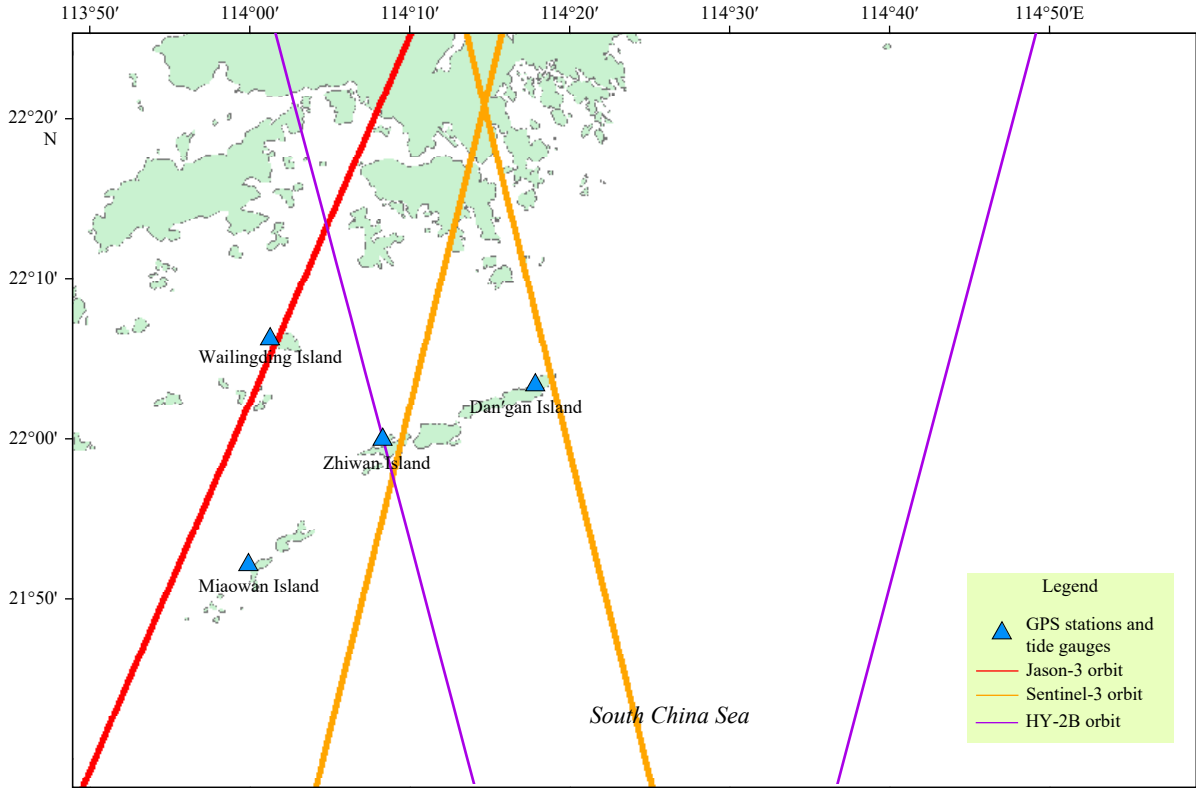


Fig. 6. The altimeters ground tracks pass the Wanshan calibration site. The purple lines are the HY-2B altimeter ground track (left line is Pass No. 375 and right one is Pass No. 362), the red line is the Jason-3 altimeter ground track, and the orange lines are the Sentinel-3A ground track.

Data Record (GDR) Version D. The bias estimates for Jason-2 GDR-D are similar to the estimates from dedicated calibration sites such as the harvest platform, the Crete site and the Bass Strait site.

Here the key equations were briefly restated. The GPS buoy calibration methodology is a direct absolute altimeter calibration. The GPS buoy was deployed at comparison point to measure the SSH when the HY-2B altimeter directly flight over the GPS buoy. In its most simplified form, the absolute altimeter SSH bias ($Bias_{alt}$) is calculated by:

$$Bias_{alt} = SSH_{alt} - SSH_{comparison\ point}, \quad (6)$$

where SSH_{alt} is the SSH calculated from the HY-2B altimeter and $SSH_{comparison\ point}$ is the SSH at the comparison point estimated from *in situ* GPS buoy measurements, which require some corrections. The SSH from the altimeter is given by:

$$SSH_{alt} = H - (R + \Delta R) - \sum Tide, \quad (7)$$

where H is the height of the satellite altimeter above the reference ellipsoid, using dual-frequency GPS for precise orbit determination. R is the range between the satellite altimeter and the sea surface, which has been corrected for altimeter instrument errors, and ΔR is the sum of the range corrections, which includes the path delay caused by the dry troposphere ΔR_{dry} and wet troposphere ΔR_{wet} , ionosphere ΔR_{iono} and effect by the sea state bias (SSB).

$$\Delta R = \Delta R_{dry} + \Delta R_{wet} + \Delta R_{iono} + SSB. \quad (8)$$

Because the SSH measured by GPS buoy includes the crustal movements caused to the ocean load tides, polar tides and solid earth, $\sum Tide$ also needs to be subtracted from SSH_{alt} .

$$\sum Tide = R_{ocean\ loading} + R_{pole\ tide} + R_{solid\ tide}, \quad (9)$$

where $R_{ocean\ loading}$, $R_{pole\ tide}$ and $R_{solid\ tide}$ are the ocean load tide, polar tide and solid earth tide, respectively. These three influencing factors have been corrected in the GPS SSH solution. Correspondingly, the satellite SSH needs to be subtracted from these three parameters.

$$SSH_{comparison\ point} = SSH_{buoy} + \Delta H_{ref\ buoy\ alt} + \Delta H_{geo}, \quad (10)$$

where SSH_{buoy} and SSH_{alt} were calculated both from same reference frame (ITRF 2008), but different reference ellipsoid parameters. So $\Delta H_{ref\ buoy\ alt}$ was used to unify to the same reference ellipsoid. ΔH_{geo} is the geoid difference between the position of HY-2B altimeter and GPS buoy.

The HY-2B altimeter orbit is designed to precision return with the ground track shift within exactly 1 km of a nominal ground track. The deployed point of the GPS buoy may not being exactly on the ground track of the HY-2B altimeter. So, the geoid difference needs to be added into Eq. (10). In this research, the WGeo model data were used, which mentioned in Section 2.1.

Finally, the equation for calculating altimeter SSH bias is given by:

$$Bias_{alt} = H - (R + \Delta R_{wet} + \Delta R_{dry} + \Delta R_{iono} + SSB) - \sum Tide - (SSH_{buoy} + \Delta H_{ref\ buoy\ alt} + \Delta H_{geo}). \quad (11)$$

3 Results

3.1 Accuracy of the WTPD

The WTPD is one of the most critical terms for the altimeter calibration site, because of the sensitivity of land contamination and the variations in water vapor near coastal areas. Use of the GPS radiosonde is one method that can measure pressure, temperature, altitude, dewpoint, wind speed and wind direction in the entire atmospheric path. In this paper, Eq. (5) given in Section 2.2.4 was used to estimate the accuracy of the WTPD for the HY-2B.

In 2018 and 2019, seven GPS radiosonde synchronization experiments were conducted. The WTPD of the CMR was compared with the GPS radiosonde and the National Centers for Environmental Prediction (NCEP) model. The results are shown in Fig. 7.

Figure 7 shows that the WTPDs by the three methods agree well. The average difference between the CMR and GPS radiosonde is -0.2 cm with a 1.4 cm STD; the difference between the CMR and NCEP model is -0.6 cm with a 1.6 cm STD; and the difference between the NCEP model and the GPS radiosonde is 0.6 cm with a 1.8 cm STD. Because the CMR lacks the first data point, the sum of the three differences is not zero. The WTPD of the CMR matches better with the GPS radiosonde. The difference of -0.2 cm indicates that the WTPD measured by the CMR is lower than the WTPD of the GPS radiosonde inversion. The target STD for the HY-2B CMR is 1.5 cm, and the STD of 1.4 cm from this assessment meets the design requirement.

In the future, if more radiosonde data are applied, including use of the Integrated Global Radiosonde Archive provided by the National Climatic Data Center, the comparison could be made

more reliable and convincing for the CMR on the HY-2B.

3.2 Absolute biases for the HY-2B

There were two HY-2B altimeter SSH calibration campaigns at the Wanshan calibration site (Table 4): one campaign took place at the start of the HY-2B satellite project for the in-orbit test from October to December 2018; another took place from September to October 2019. A total of eight *in situ* absolute calibration experiments have been conducted in those campaigns using the GPS buoy.

Distance (Row 5 in Table 4) represents the distance from the GPS buoy placed at the sub-satellite point of the satellite orbit to the GPS reference station. The GPS buoy was placed within 1 km of the satellite's nadir point, and the GPS reference station was set up on the island. The distance between the GPS buoy and the GPS reference station is a compromise, which needs to take into account both the GPS solution accuracy (shorter distance) and altimeter measurement validity (longer distance).

HY-2B took over the HY-2A missions in 2018. The HY-2B altimeter's SSH data used in this research were Level 2 IGDR products distributed by NSOAS; the SSH has still not been calibrated absolutely at an operational calibration site. In this research, the main altimeter range correction terms were processed before Eq. (10) was used to calculate the absolute bias.

The processing strategies for the main altimeter range correction terms for the Wanshan calibration site were similar to the strategies used at other dedicated calibration sites, but certain aspects of the strategies were unique to the Wanshan site. Details are given in Table 5.

Pass No. 362 at the Wanshan calibration site is a descending track and Pass No. 375 is an ascending pass track, so the pro-

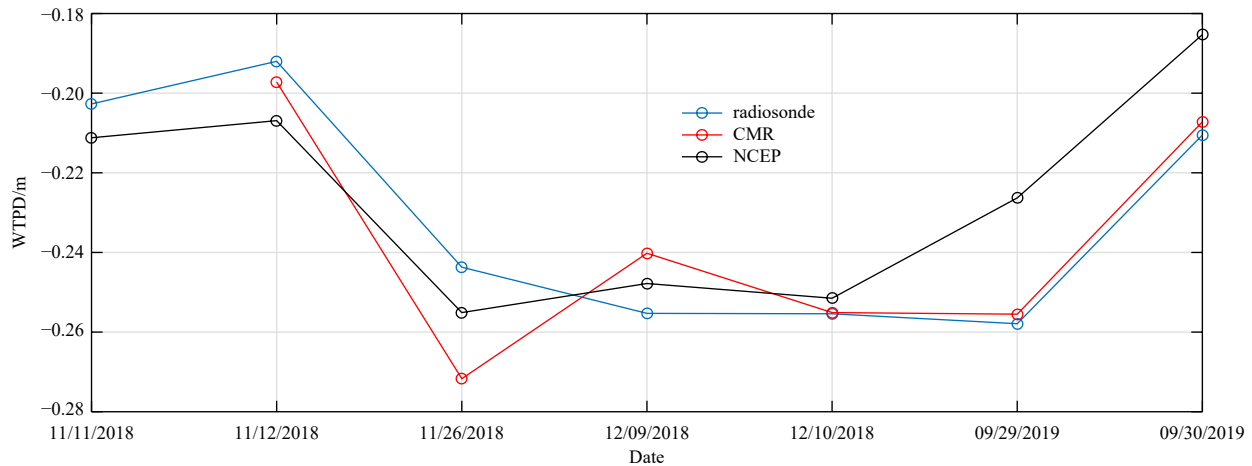


Fig. 7. Wet troposphere path delay (WTPD) measured by the CMR, radiosonde and NCEP model. CMR: correction microwave radiometer, NCEP: National Centers for Environmental Prediction.

Table 4. Absolute calibration results for HY-2B SSH using the GPS buoy

Time (UTC)	Cycle	Pass No.	Position	Distance/km	Bias/cm
11/11/2018	0001	362	east of DG	43.4	25.38
11/12/2018	0001	375	south of ZW	22.8	19.95
11/25/2018	0002	362	east of DG	41.2	2.65
11/26/2018	0002	375	south of ZW	22.1	2.46
12/09/2018	0003	362	east of DG	37.1	1.54
12/10/2018	0003	375	south of ZW	22.3	4.01
09/29/2019	0024	362	east of DG	41.6	6.80
09/30/2019	0024	375	south of ZW	17.4	-0.10

cessing strategies of the main altimeter range correction terms are different. GPS radiosonde data are the priority for the WTPD; otherwise, the CMR data are used for range correction. The dry troposphere path delay (DTPD) corrections were also evaluated comparing with local pressure. And the difference between HY-2B IGDR and calculated by *in situ* atmospheric pressure was negligible.

Using the GPS buoy calibration methodology, the absolute bias of the HY-2B altimeter SSH varied from 25.38 cm to -0.1 cm (Table 4). Removing two anomalous data items from cycle 0001 (two red diamond points in Fig. 8), the time-averaged bias for the HY-2B altimeter’s SSH was approximately 2.89 cm with a 2.35 cm STD. Due to the difference in distance (between the GPS buoy and the GPS reference station), the calibration results of the two passes were calculated separately. The time-averaged bias for HY-2B altimeter’s Pass No. 375 SSH was approximately 2.12 cm with a 2.08 cm STD, and 3.66 cm with a 2.77 cm STD for HY-2B altimeter’s Pass No. 362 SSH. Pass No. 362 is inferior to Pass No. 375 for calibration because it is further from the calibration site, so the calibration result of Pass No. 375, bias 2.12 cm with 2.08 cm STD, was treated as the GPS buoy calibration result of the HY-2B Altimeter’s SSH at China’s Wanshan calibration site.

4 Discussion

Before using the GPS calibration method to calibrate the satellite altimeter SSH, the accuracy of GPS buoy measurement needs to be evaluated. The Bass Strait site presented the error budget for MK II GPS buoy deployments for the bias calculation were derived from a single overflight at the 4.0–4.5 cm level (Watson et al., 2003). Comparing with the tide gauge, the STD of the new style GPS buoy at Bass Strait site was 2.4 cm (Watson et al., 2019). The total error budget estimate for the SSH measured at the Wanshan GPS buoy was almost 2.7 cm, which is better than

the Mk II GPS buoy and similar with new style GPS buoy of Bass Strait calibration site. The assessment verified that the GPS buoy calibration methodology used at the Wanshan calibration site is feasible, reliable and accurate, and can be used for altimeter SSH calibration.

Using a GPS buoy calibration method, the accuracy of SSH data for the HY-2B altimeter has been preliminary assessed in two campaigns. The HY-2B SSH absolute biases for cycle 0001 were anomalous, as shown in Fig. 8. The GPS buoy used in this research has been verified through many experiments since 2013, including a water level test in the lab, static accuracy experiments at different distances from reference stations in a reservoir, contrast experiments with a tide gauge near the coast and Jason-2 and HY-2A altimeter SSH calibration experiments at Qinglan Port (Chen et al., 2019). All these experiments verified the accuracy and stability of the GPS buoy calibration methodology. The anomalous biases seen in Fig. 8, 25 cm for cycle 0001 Pass No. 362 and 19 cm for cycle 0001 Pass No. 375, may not have been caused by the GPS buoy. There were two reasons for us to show these two abnormal results. On one hand, there is a problem with the satellite altimeter SSH in the cycle 0001. Everyone needs to pay attention when using the HY-2B altimeter cycle 0001 data. On the other hand, the problem was raised for the relevant departments to study, for example the precision orbit determination department and altimeter data processing department, which can improve altimeter satellite data processing.

The data for HY-2B altimeter cycle 0001 Pass No. 362 and Pass No. 375 were carefully analyzed. The altitude range, dry troposphere correction, wet troposphere correction, ionosphere correction, Sea State Bias (SSB), ocean load tide, solid earth tide and pole tide have all been examined. Taken the variation of HY-2B cycle 0001 cycle SSH as example, there were no significant change in the comparison points (Fig. 9). So, the reason for the

Table 5. Processing strategies for the HY-2B Altimeter SSH at Wanshan calibration site

Correction	Processing strategies
Ionosphere	mean over -20 s to the TCA for the Pass No. 375; mean over the TCA to 20 s for the Pass No. 362
Dry troposphere	linear fit of 3 data either side of the HY-2B altimeter comparison point, interpolated to the TCA
Wet troposphere	use the GPS radiosonde data or linear fit over -10 s to TCA for the Pass No. 375; linear fit over the TCA to 10 s for the Pass No. 362, interpolated to the TCA
Sea State Bias	cubic fit over -10 s to the TCA for the Pass No. 375; cubic fit over the TCA to 10 s for the Pass No. 362, interpolated to the TCA

Note: TCA represents time of closest approach.

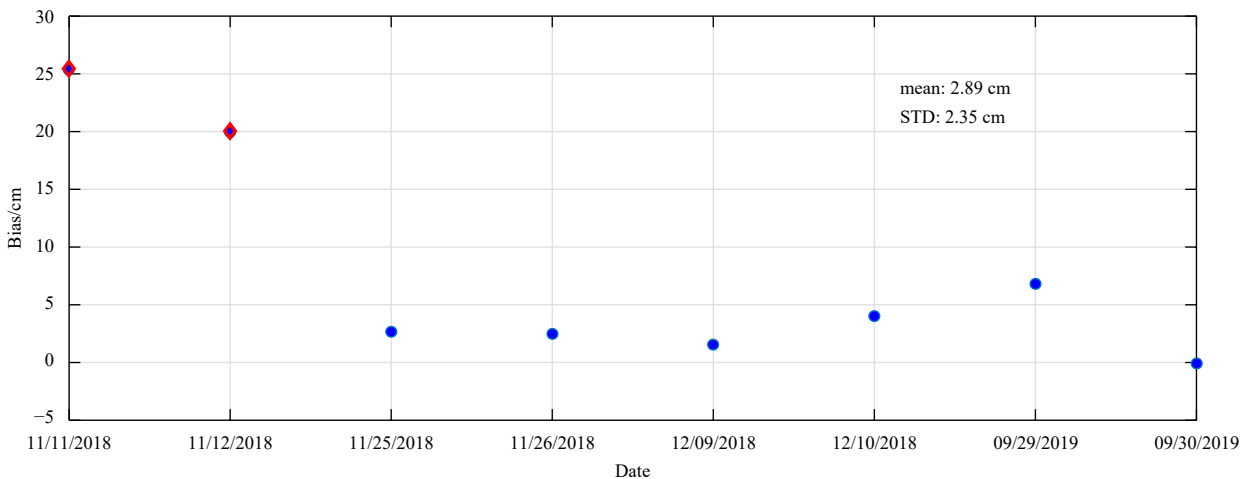


Fig. 8. Bias of HY-2B altimeter SSH with the GPS buoy calibration method.

20-cm bias has yet to be detected. And now the HY-2B altimeter data from cycle 0001 to cycle 0006 are still in reprocessing. The precise HY-2B orbit and the instrument’s error will be analyzed by researchers at NSOAS and us.

The accuracy of the CMR’s WTPD was also assessed using the *in situ* GPS radiosonde. The accuracy was a -0.2 cm bias with a 1.4 cm STD compared to the GPS radiosonde, and a -0.6 cm bias with a 1.62 cm STD compared with the NCEP. The accuracy of Sentinel-3A’s WTPD was a -2.3 cm bias with a 1.5 cm STD compared with the GPS at the Corsica calibration site (Table 6). The accuracy of the AMR’s WTPD (GDR-D) on Jason-2 was a 0.32 cm bias with a 1.24 cm STD and for Jason-3’s AMR (GDR-T), and was a 0.26 cm bias with a 1.2 cm STD compared with the GPS at the Corsica calibration site (Bonnetfond et al., 2017). The CMR’s WTPD on the HY-2B had a similar accuracy level to the AMR on Sentinel-3A and Jason-2/3.

The calibration method for the Wanshan calibration site was similar to the other dedicated calibration sites, but certain aspects of the data process strategies were unique. The HY-2B SSH data processing methods were established separately for HY-2B ascending track and descending track, which formed the unique calibration data processing strategy of Wanshan calibration field. The estimated accuracy of the HY-2B altimeter’s SSH was a 2.12 cm bias with a 2.08 cm STD excluding the cycle 0001 biases at the Wanshan calibration site. The accuracy of Jason-2’s SSH (GDR-D) was a 1.6 cm bias with a 3.3 cm STD and Jason-3’s SSH (GDR-

T) was a -0.7 cm bias with a 3.0 cm STD at the Corsica calibration site (Bonnetfond et al., 2017). The average bias for Jason-2’s SSH was 0.48 cm and -0.62 cm for Jason-3 (GDR-D) at the Gavdos calibration site (Mertikas et al., 2018). The latest absolute calibration results of Jason-2 and Jason-3 altimeters in the four calibration fields have been listed in Table 7. The absolute bias of HY-2B SSH was higher than Jason-2 and Jason-3, that caused by the less statistical data at Wanshan calibration site. The STD of the HY-2B altimeter’s SSH at the Wanshan calibration site agrees well with the accuracy for Jason-2 and Jason-3 at the Corsica, Gavdos, Harvest and Bass Strait calibration sites.

Through the study, the feasibility of GPS calibration method in Wanshan calibration field is proved, and the preliminary calibration results of HY-2B altimeter SSH have been carried out. The results show that HY-2B is on the same accuracy level as the international operational altimeters.

5 Conclusions

The major *in situ* observation instruments of Wanshan calibration site have been built up. Wanshan calibration field conducted trial operation from December 2019 to February 2020, and the other instruments such as mooring GPS buoy and pressurized tide gauge will deploy soon. This paper made an error budget analysis of the GPS calibration method of Wanshan calibration site, and used the comparison experiment to evaluate the accuracy of GPS buoy. The accuracy of the two methods (Section

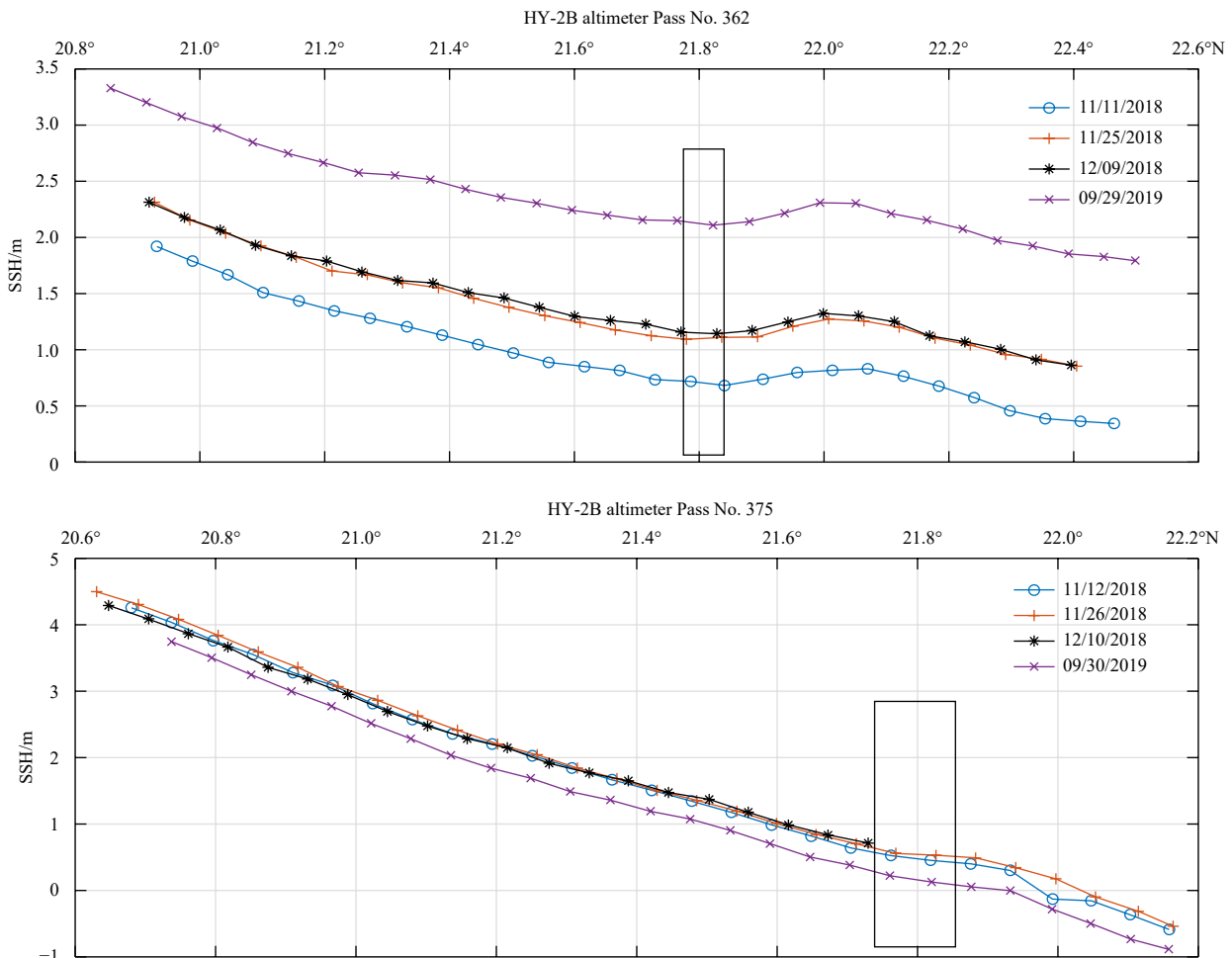


Fig. 9. The HY-2B altimeter SSH at Wanshan calibration site. The positions of boxes were the comparison points.

Table 6. WTPD correction differences in the calibration sites

Calibration site	Altimeter	Bias/cm	STD/cm
Wanshan	HY-2B IGDR	-0.20	1.40
Corsica (Bonnetfond et al., 2017)	Jason-2 GDR-D	0.32	1.24
	Jason-3 GDR-T	0.26	1.20
	Sentinel-3A	2.30	1.50
Harvest (Haines et al., 2019)	Jason-2 GDR-D	-0.47	0.80
	Jason-3 GDR-D	-0.33	0.85

Table 7. The accuracy of altimeter SSH in the calibration sites

Calibration site	Altimeter	Bias/cm	STD/cm
Wanshan	HY-2B IGDR	2.12	2.08
Corsica (Bonnetfond et al., 2017)	Jason-2 GDR-D	1.60	3.3
	Jason-3 GDR-T	-0.70	3.0
Gavdos (Mertikas et al., 2018)	Jason-2 GDR-D	0.48	-
	Jason-3 GDR-D	-0.62	-
Harvest (Haines et al., 2019)	Jason-2 GDR-D	0.50	3.2
	Jason-3 GDR-D	1.50	2.7
Bass Strait (Watson et al., 2019)		1.90	3.2 (TG)
	Jason-2 GDR-D	1.80	2.5 (Mooring)
	Jason-3 GDR-D	-0.62	3.0 (TG)
		-0.85	2.6 (Mooring)

Note: - represents no data. TG: calibration result from tide gauge. Mooring: calibration result from mooring deployments.

2.2.2) is close, better than 2.7 cm, which showed the reliability and accuracy of the GPS buoy method at Wanshan calibration site, and provides a basis for the follow-up mooring GPS buoy calibration method.

The wet path delay correction is one of the main sources of error in altimeter SSH measurement, and is also an important factor at the altimeter calibration site. The *in situ* radiosonde data have been used to carry out the accuracy evaluation of HY-2B CMR WTPD. The results showed that the accuracy of HY-2B CMR WTPD is 1.4 cm, which met the design specification of HY-2B CMR.

Using a GPS buoy, the preliminary accuracy of SSH data for the HY-2B altimeter has been assessed in two campaigns with six simultaneous *in situ* measurements and HY-2B altimeter. The calibration results showed that the average bias of HY-2B altimeter is 2.12 cm with 2.08 cm STD. Compared with Jason-2 and Jason-3 accuracy in the four absolute, permanent and calibration sites, the accuracy of HY-2B altimeter SSH is close to mainstream altimeters' accuracy.

Although the absolute bias for the HY-2B from these two campaigns was determined from a small sample (eight GPS buoy measurements), the results verify the feasibility and reliability of the GPS buoy calibration methodology used at the Wanshan calibration site. More *in situ* calibration experiments are necessary to calibrate the HY-2B's SSH. Combined instrumentation consisting of a GPS buoy, mooring GPS buoy and tide gauges will be installed at the Wanshan calibration site. Together, the measurements by the GPS buoy, mooring GPS buoy and tide gauges can provide a unique *in situ* observation data set for determining the altimeter SSH bias and bias drift at the Wanshan calibration site.

Acknowledgements

We thank Youguang Zhang, Zhenzhan Wang, Bonnetfond P, Xiyu Xu, Hua Shen, Zengrui Rong, Yanlong Liu, Xiaoxu Zhang and Qian Zhang for useful discussions. We also thank the NSOAS

of MNR for providing HY-2B RA IGDR data. We thank Michael Luetchford, BTEch, from Liwen Bianji, Edanz Group China (www.liwenbianji.cn/ac), for editing the English text of a draft of this manuscript.

References

- Bonnetfond P, Exertier P, Laurain O, et al. 2003a. Absolute calibration of Jason-1 and TOPEX/Poseidon altimeters in Corsica. *Marine Geodesy*, 26(3-4): 261-284
- Bonnetfond P, Exertier P, Laurain O, et al. 2003b. Leveling the Sea surface using a GPS-catamaran. *Marine Geodesy*, 26(3-4): 319-334
- Bonnetfond P, Exertier P, Laurain O, et al. 2010. Absolute calibration of Jason-1 and Jason-2 altimeters in Corsica during the formation flight phase. *Marine Geodesy*, 33(S1): 80-90
- Bonnetfond P, Exertier P, Laurain O, et al. 2015. SARAL/AltiKa absolute calibration from the multi-mission Corsica facilities. *Marine Geodesy*, 38(S1): 171-192
- Bonnetfond P, Exertier P, Laurain O, et al. 2017. Corsica: a multi-mission absolute calibration site. In: *Proceedings of 2017 OSTST Meeting*. La Miami, USA: OSTST
- Bonnetfond P, Exertier P, Laurain O, et al. 2018. Calibrating the SAR SSH of Sentinel-3A and CryoSat-2 over the Corsica Facilities. *Remote Sensing*, 10(1): 92
- Brown S. 2010. A novel near-land radiometer wet path-delay retrieval algorithm: application to the Jason-2/OSTM advanced microwave radiometer. *IEEE Transactions on Geoscience and Remote Sensing*, 48(4): 1986-1992, doi: [10.1109/TGRS.2009.2037220](https://doi.org/10.1109/TGRS.2009.2037220)
- Brown S, Ruf C, Keihm S, et al. 2004. Jason microwave radiometer performance and on-orbit calibration. *Marine Geodesy*, 27(1-2): 199-220
- Cancet M, Bijac S, Chimot J, et al. 2013. Regional *in situ* validation of satellite altimeters: calibration and cross-calibration results at the Corsican sites. *Advances in Space Research*, 51(8): 1400-1417, doi: [10.1016/j.asr.2012.06.017](https://doi.org/10.1016/j.asr.2012.06.017)
- Chen Chuntao. 2010. Using multi-sensor satellite data to study the variability of Kuroshio (in Chinese) [dissertation]. Qingdao: Ocean University of China
- Chen Chuntao, Zhai Wanlin, Yan Longhao, et al. 2014. Assessment of the GPS buoy accuracy for altimeter sea surface height calibration. In: *Proceedings of 2014 IEEE Geoscience and Remote Sensing Symposium*. Quebec: IEEE, 3101-3104
- Chen Chuntao, Zhu Jianhua, Zhai Wanlin, et al. 2019. Absolute calibration of HY-2A and Jason-2 Altimeters for sea surface height using GPS buoy in Qinglan, China. *Journal of Oceanology and Limnology*, 37(5): 1533-1541, doi: [10.1007/s00343-019-8216-8](https://doi.org/10.1007/s00343-019-8216-8)
- CLS. 2013. Jason-2 validation and cross calibration activities (Annual report 2012). http://www.avisio.altimetry.fr/fileadmin/documents/calval/validation_report/J2/annual_report_j2_2012.pdf [2013-03-26]
- Estey L, Wier S. 2013. Teqc tutorial basics of teqc use and teqc products. Boulder: UNAVCO
- Frappart F, Roussel N, Biancale R, et al. 2015. The 2013 Ibiza calibration campaign of Jason-2 and SARAL altimeters. *Marine Geodesy*, 38(S1): 219-232, doi: [10.1080/01490419.2015.1008711](https://doi.org/10.1080/01490419.2015.1008711)
- Fu L L, Cazenave A. 2001. *Satellite Altimetry and Earth Sciences: A Handbook of Techniques and Applications*. San Diego: Academic Press, 407-435
- Haines B J, Desai S D, Born G H. 2010. The harvest experiment: calibration of the climate data record from TOPEX/Poseidon, Jason-1 and the ocean surface topography mission. *Marine Geodesy*, 33(S1): 91-113
- Haines B, Desai S, Dodge A, et al. 2019. The harvest experiment: new results from the platform and moored GPS buoys. In: *Proceedings of 2019 Ocean Surface Topography Science Team Meeting*. Chicago, USA: OSTST. https://meetings.avisio.altimetry.fr/fileadmin/user_upload/2019/CVL_02_calval_harv_haines.pdf
- Haines B, Desai S, Shah R, et al. 2016. The Harvest experiment: connecting Jason-3 to the long-term sea level record. In: *Proceedings of Ocean Surface Topography Science Team Meeting 2016*.

- La Rochelle, France. https://meetings.aviso.altimetry.fr/fileadmin/user_upload/tx_ausyclsseminar/files/CVL_02_Haines_harvest_14h15.pdf
- Herring T A. 2002. TRACK GPS Kinematic Positioning Program, Version 1.07. Massachusetts: Massachusetts Institute of Technology
- Herring T A, King R W, Folyd M A, et al. 2018a. GPS Analysis at MIT Release 10.7. Cambridge: Massachusetts Institute of Technology
- Herring T A, King R W, Floyd M A, et al. 2018b. Introduction to GAMIT/GLOBK Release 10.7. Cambridge: Massachusetts Institute of Technology
- Keihm S J, Janssen M A, Ruf C S. 1995. TOPEX/Poseidon microwave radiometer (TMR). III. Wet troposphere range correction algorithm and pre-launch error budget. *IEEE Transactions on Geoscience and Remote Sensing*, 33(1): 147–161, doi: [10.1109/36.368213](https://doi.org/10.1109/36.368213)
- King R W, Bock Y. 2005. Documentation for the GAMIT GPS analysis software, release 10. Cambridge: Massachusetts Institute of Technology
- Lin Mingsen, He Xianqiang, Jia Yongjun, et al. 2019. Advances in marine satellite remote sensing technology in China. *Haiyang Xuebao*, 41(10): 99–112, doi: [10.3969/j.issn.0253-4193.2019.10.006](https://doi.org/10.3969/j.issn.0253-4193.2019.10.006)
- Ma Yue, Xu Nan, Liu Zhen, et al. 2020. Satellite-derived bathymetry using the ICESat-2 lidar and Sentinel-2 imagery datasets. *Remote Sensing of Environment*, 250: 112047, doi: [10.1016/j.rse.2020.112047](https://doi.org/10.1016/j.rse.2020.112047)
- Mertikas S P, Donlon C, Féménias P, et al. 2018. Fifteen years of Cal/Val Service to reference altimetry missions: calibration of satellite altimetry at the permanent facilities in Gavdos and Crete, Greece. *Remote Sensing*, 10(10): 1557, doi: [10.3390/rs10101557](https://doi.org/10.3390/rs10101557)
- Mertikas S P, Donlon C, Mavrocordatos I N, et al. 2016. Gavdos/West Crete Cal-val site: Over a decade calibrations for altimetry. In: *Proceedings of 2016 Ocean Surface Topography Science Team Meeting*. La Rochelle, France: Centre national d'études spatiales
- Mertikas S P, Ioannides R T, Tziavos I N, et al. 2010. Statistical models and latest results in the determination of the absolute bias for the radar altimeters of Jason satellites using the Gavdos facility. *Marine Geodesy*, 33(S1): 114–149
- Watson C, Coleman R, White N, et al. 2003. Absolute calibration of TOPEX/Poseidon and Jason-1 using GPS buoys in Bass Strait, Australia. *Marine Geodesy*, 26(3–4): 285–304
- Watson C, Legresy B, Beardsley J, et al. 2019. Absolute altimeter bias results from Bass Strait, Australia. In: *Proceedings of 2019 OSTST Meeting*. Chicago, USA: OSTST
- Watson C, Legresy B, King M, et al. 2016. Altimeter absolute bias estimates from Bass Strait, Australia. In: *Proceedings of 2016 Ocean Surface Topography Science Team Meeting*. La Rochelle, France: Centre national d'études spatiales
- Watson C, White N, Church J, et al. 2011. Absolute calibration in Bass Strait, Australia: TOPEX, Jason-1 and OSTM/Jason-2. *Marine Geodesy*, 34(3–4): 242–260
- Zhai Wanlin, Zhu Jianhua, Ma Chaofei, et al. 2020. Measurement of the sea surface using a GPS towing-body in Wanshan area. *Acta Oceanologica Sinica*, 39(5): 123–132, doi: [10.1007/s13131-020-1599-8](https://doi.org/10.1007/s13131-020-1599-8)
- Zheng Gang, Yang Jingsong, Ren Lin. 2014. Retrieval models of water vapor and wet tropospheric path delay for the HY-2A calibration microwave radiometer. *Journal of Atmospheric and Oceanic Technology*, 31(7): 1516–1528, doi: [10.1175/JTECH-D-14-00005.1](https://doi.org/10.1175/JTECH-D-14-00005.1)